

Chapter 2

Aerosol Forcing and the A-Train

CHIP TREPTE

Introduction

Aerosols are small particles consisting of solid or liquid material suspended in air, with diameters ranging from about 0.01 to 1 μm . They originate primarily from natural sources such as volcanoes, dust storms, forest fires, vegetation, and sea spray. Anthropogenic sources include burning of fossil fuels and land use changes such as biomass burning and deforestation. Depending upon their size, injection altitude, and proximity to precipitating cloud systems, lifetimes of aerosols in the atmosphere vary considerably from a few hours to as much as 2 weeks and thus, can be transported long distances from their sources.

Aerosols can have a significant impact on the environment and climate. They can have a *direct* radiative forcing effect by scattering and absorbing sunlight. The change in direct radiative forcing due to anthropogenic aerosols alone (also known as direct aerosol climate forcing) is substantial and rivals that due to stable greenhouse gases. For the most part it is opposite in sign to the greenhouse gases, however, the regional nature of aerosol forcing and its variable vertical distribution precludes simple conclusions of a global canceling of greenhouse gas warming.

Aerosols can also *indirectly* influence radiative forcing by modifying the albedo of clouds either through the incorporation of absorbing aerosols, which tend to darken them, or through the seeding of smaller droplets, which tend to brighten them. It has been suggested that aerosols can alter the liquid water content of clouds, thereby lengthening cloud lifetime and the geographical extent of cloudiness, or even change the vertical structure of latent heating and influence atmospheric dynamics.

At present, our ability to quantify and predict the impact of global aerosol forcing on climate remains highly uncertain [IPCC, 2001]. The uncertainties arise, in part, because of insufficient knowledge of aerosol variability, composition, optical properties, hygroscopicity, and size distribution. Complex aerosol processes such as transport, transformation, aging, and cloud interactions are also poorly represented in models. More observations from a variety of techniques, platforms, and

vantage points are needed to improve our characterization of the aerosol system and reduce modeling uncertainties.

In the next 12 months, the A-train satellite constellation consisting of the Aqua, CloudSat, CALIPSO, PARASOL, and Aura satellite missions will be fully assembled in orbit and will provide valuable new information to help address some of these uncertainties. For the first time, a three-dimensional view of the aerosol and cloud system over the globe will be available from a combined instrument suite including a lidar, a radar, multispectral imagers and broadband radiometers. These measurements will enable more accurate estimates of direct aerosol forcing than presently available. They will be made above, below, and next to cloud systems; over bright and dark surfaces; and at high and low latitudes. The measurement suite will further permit a better understanding of regional impacts of indirect aerosol forcing and the evolution of aerosol distributions that will help to constrain parameterizations of aerosol processes in climate models.

This lecture will provide an overview of the basic factors governing direct and indirect aerosol radiative forcing. It will be followed with a summary of the measurement capabilities for aerosols on the A-Train constellation and on how these might be utilized to better understand aerosol processes and provide more accurate estimates of aerosol forcing.

Direct Aerosol Forcing

In the early 1990s it was believed that radiative forcing by tropospheric aerosols was dominated by sulfate droplets such as those found in the stratosphere following large volcanic eruptions. These aerosols absorbed negligible amounts of visible light and, hence, have a single scattering albedo (fraction of light attenuated by scattering to the total amount attenuated by scattering and absorption) close to unity [Charlson et al., 1992]. Over the years, however, greater realization of the importance of different aerosol types and their optical properties revealed that aerosol forcing is more complicated and may, under suitable conditions, cause net heating.

The following expression [Haywood and Shine, 1995] is used to identify how different factors influence aerosol radiative forcing:

$$\Delta F = -DS_oT_{at}^2(1 - A_c)\omega\beta\delta\left((1 - R_s)^2 - \frac{2R_s}{\beta}\left(\frac{1}{\omega} - 1\right)\right)$$

where D is daylight, S_o is the solar constant, T_{at} is the atmospheric transmission above the aerosol layer, A_c is fractional cloud cover, R_s is the surface reflectivity, ω is the single scattering albedo (fraction of light attenuated by scattering to the total amount attenuated by both absorption and scattering), δ is optical depth, and the β is the upscatter fraction. The expression reveals that in clear skies ΔF is governed principally by aerosol abundance through δ , aerosol optical properties through β and ω , and the underlying surface reflectance.

Further inspection of the above equation reveals that forcing can shift from net cooling to net warming when

$$\omega < \frac{2R_s}{\beta(1 - R_s)^2 + 2R_s}$$

Typical values of the upscatter fraction β range from .15 to .30. For sulfate aerosols ($\omega \sim 1$), the radiative forcing is negative over almost all surface conditions. However, for aerosols that absorb solar radiation (e.g., containing black carbon) the single scattering coefficient decreases, net warming occurs when the particles overlie gray or bright surfaces. For example, when $\omega = 0.9$ and $R_s > 0.3$, the atmosphere will warm. This example is simplified to illustrate a few of the complexities involved in modeling direct aerosol forcing. More accurate representation would include factors with possible interdependencies such as hygroscopicity, internal/external mixtures, varying solar angles, etc.

Since climate forcing is due only to the anthropogenic component of the aerosol distribution, we need isolate this contribution from the total radiative forcing calculation. This aspect is best performed by chemical analysis with in situ instrument probes. An upper estimate of global climate forcing from satellite observations may be obtained by realizing that anthropogenic aerosols often fall within the fine mode fraction as suggested by a conceptual representation of the aerosol size distribution. Coarse mode particles are usually formed by mechanical actions (e.g., wind-blown dust or sea salt). Fine mode particles often form as a result of combustion or nucleation/condensation. The difficulties of isolating the anthropogenic component and the need for global observations underlines the need for an integrated measurement sensor web that includes ground-base, aircraft, satellite observations fused together by data assimilation techniques [Diner et al., 2004; Anderson et al., 2004].

Indirect Aerosol Forcing

Since aerosols are the building blocks of clouds, it is natural to expect that changes in aerosol characteristics can impact the properties of clouds. Twomey [1977] first described how the presence of more cloud condensation nuclei could increase the liquid water content (LWC) of clouds and change their cloud optical properties.

To illustrate the relationship, consider the definition of optical depth,

$$\delta = \pi h \int_0^\infty Q_e r^2 n(r) dr$$

where h is the depth of the cloud, Q_e is the extinction efficiency, r is the particle radius, and $n(r)$ is the size distribution. At visible wavelengths $Q_e \sim 2$. If we further consider a narrow droplet-size spectrum with a mean radius, \bar{r} , the above expression can be approximated as

$$\delta = 2\pi h \bar{r}^2 N$$

where

$$N = \int_0^\infty n(r) dr$$

is the total number concentration of droplets. The total liquid water content of a cloud is defined as

$$LWC = \frac{4\pi}{3} \rho \int_0^\infty r^3 n(r) dr$$

After making similar substitutions for the droplet size distribution and mean radius the expression can be approximated by

$$LWC = \frac{4\pi}{3} \rho \bar{r}^3 N$$

Relating together the approximated expressions for optical depth and liquid water content yields

$$\delta = 2.4 \left(\frac{LWC}{\rho} \right)^{2/3} h N$$

This has the consequence that an increase in cloud condensation nuclei produces an increase in optical thickness. Because of the increased competition for water vapor with the increased aerosol population, cloud droplets may be unable to grow large enough to initiate the collision-coalescence process (the dominate precipitation process for warm clouds). The prevailing thought is that precipitation rates, thus, will decrease and cloud lifetimes lengthen.

A number of studies have observed changes in aerosol concentrations, cloud droplet number/size, and cloud reflectance. Many of these studies include both aircraft and satellite observations at near-infrared wavelengths, where cloud reflectance is highly sensitive to droplet size rather than optical thickness [e.g., Nakajima et al., 2001]. Some of the most compelling evidence showing changes in aerosol optical properties by aerosol concentration comes from AVHRR observations of the effects of ship exhaust on clouds [Coakley et al., 1987]. Because of the magnitude and degree of uncertainty with indirect aerosol forcing, more observations and more modeling research is needed. Further investigations from the advantage point of space, hopefully, can continue to provide an improved understanding of the regional and global affects of aerosol-cloud interactions and their impact on climate.

A-Train Aerosol Measurements

The A-Train satellite constellation (named for the Aqua and Aura satellites) has an orbit at an altitude of 705 km and inclination of $\sim 98^\circ$. Aqua leads the constellation with an equatorial crossing time of approximately 1:30 p.m. and Aura trails the set with a crossing time of $\sim 1:45$ p.m. On December 2004, the PARASOL satellite was launched followed by the joint launch of CALIPSO and CloudSat on April 2006. These satellites have been joined the constellation in orbit between the Aqua and Aura platforms. Table 1 summarizes the instruments on the different platforms and products available for aerosol studies. As seen in the table, a large number of near-coincident measurements on aerosol and cloud physical and optical properties, radiative flux, and thermodynamic parameters will be available over the same locations within a few minutes of each other. (Details on the

A-train constellation may be found at the following Web site: http://eospsso.gsfc.nasa.gov/eos_homepage/for_educators/educational_publications.php.)

Global maps of aerosol optical depth can be derived from measurements by MODIS, PARASOL and OMI. These instruments exploit the spectral sensitivity of the size distribution and composition of aerosols to infer their optical properties. For MODIS, visible and near-IR measurements over dark surfaces are used to retrieve aerosol optical depth [Kaufman et al., 2002] and provide discrimination between accumulation and coarse size modes [Remer et al., 2002]. Over bright surfaces, less spectral information is available because of the lack of spectral contrast and the complications of large variability in surface bidirectional reflectance. An example map of aerosol optical depth derived from MODIS is shown in Figure 1 for the months of January and July 2003. For the month of January, most oceanic regions have $\delta < 0.2$. However, near the western coast of Africa and over central Africa values peak around 0.8. High values are also present over eastern China. For the month of July, much higher aerosol loading is present over the globe with peaks in regions near or downwind of the major deserts and large areas of industrial activity. The white regions in both figures are data void areas (note that they occur over high albedo regions). It should be noted that application of the technique is permitted only for cloud free pixels. The data shown represents the cumulative average for available scenes for the month. These were obtained from a catalogue of aerosol data products from the MODIS Online Visualization and Analysis System at (http://lake.nascom.nasa.gov/www/online_analysis/movas).

Aerosol retrievals using POLDER observations on PARASOL are expected to follow the technique demonstrated Bellouin et al. [2003]. The approach uses multi-angle images at 9 different wavelengths (443, 490, 565, 670, 763, 765, 865, 910, and 1020 nm) with channels at 490, 670, and 865 nm sensitive to polarized signals to derive optical depth and information on aerosol size distribution (Angstrom coefficient) over the ocean. Over land, the technique provides an index that is proportional to the product of optical depth and the Angstrom coefficient. The OMI aerosol retrieval uses near-UV spectral channels instead of those used by MODIS in the mid-visible region. The advantage in this approach is that most land surfaces are dark in the near UV and the interaction between aerosol and Rayleigh scattering offers sensitivity to aerosol absorption [Torres et al., 2002]. This feature permits OMI to provide insight on the bulk distribution of single scattering albedo over the globe.

The addition of CALIPSO mission to the A-train constellation greatly complements the other aerosol observations by providing information on the vertical structure of aerosol and cloud layers [Winker et al., 2003]. CALIPSO consists of a polarization-sensitive lidar operating at 1064 and 532 nm and passive imagers operating in the visible and infrared spectral regions. It has a designed optical depth sensitivity of at least 0.005 at 532 nm. With this information, aerosol features can be unambiguously identified above and between clouds and over bright surfaces. The technique is especially sensitive at low optical depths and promises

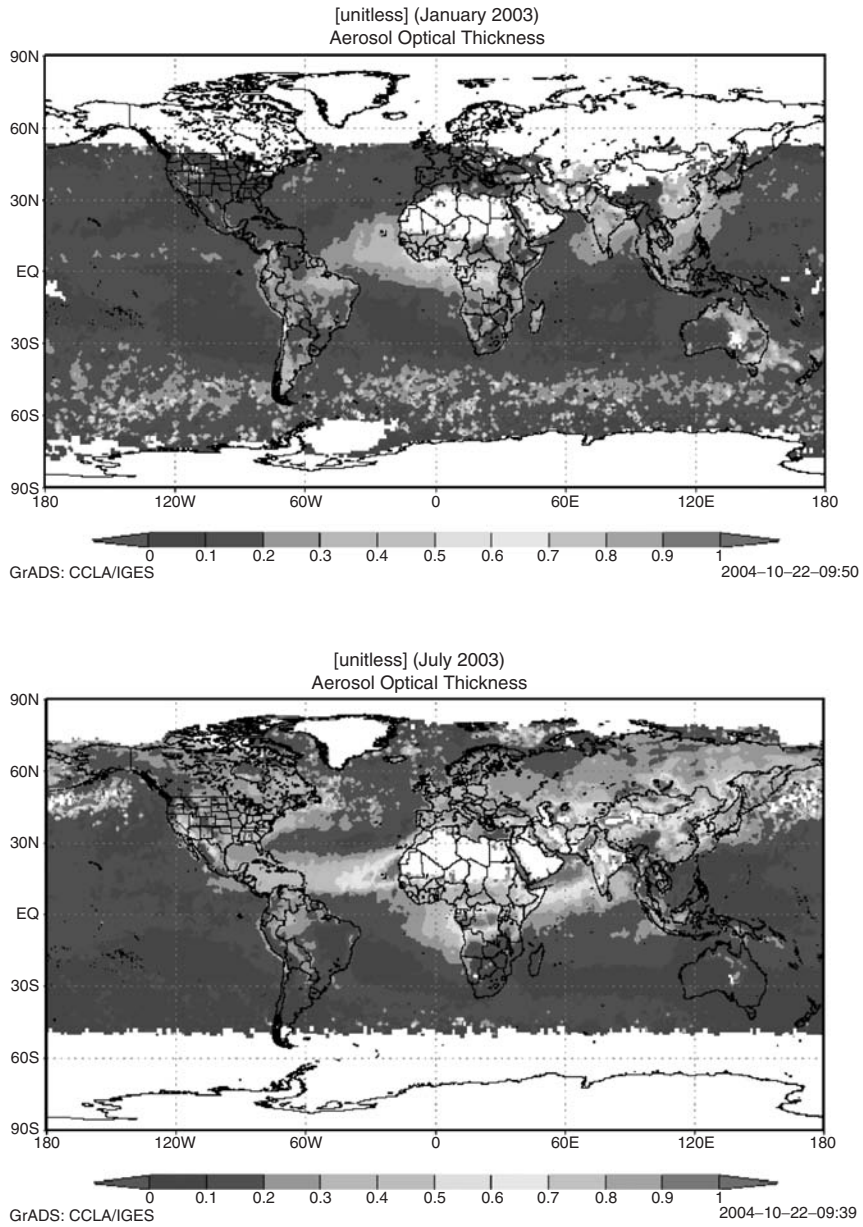


FIGURE 1. Aerosol optical depth obtained from the MODIS satellite experiment for the months of January and July 2003.

to improve our quantitative estimate of global aerosol forcing. This is illustrated in Figure 2, which shows the estimated uncertainty derived from CALIPSO compared with retrievals from MODIS. At low optical depths ($< \sim 0.2$), lidar retrievals are superior. Their accuracy degrades at higher optical depths because of greater weighting in the uncertainty of the extinction-to-backscatter coefficient that is used in the aerosol retrieval algorithm. This parameter is dependent on composition and the size distribution.

CALIPSO's measurements of aerosol layers will also be valuable in evaluating model transport processes. It is widely recognized that chemical-transport models still have difficulty in reproducing observed vertical distributions of aerosols. The ability to distinguish aerosol layers within or above the boundary layer will help to identify transport pathways and provide insight on their region of origin with the use of backtrajectory analysis and tracer observations. An example of a set of lidar observations is shown in Figure 3 from the LITE experiment, which flew on the Space Shuttle in 1994. In this figure, the vertical structure of clouds and aerosols are clearly evident. The yellow lines show backtrajectories and highlight the nature of differential transport processes in the atmosphere.

Another area where the CALIPSO data will provide new information is in the use of the ratio of 532/1064-nm backscatter measurements. According to Mie

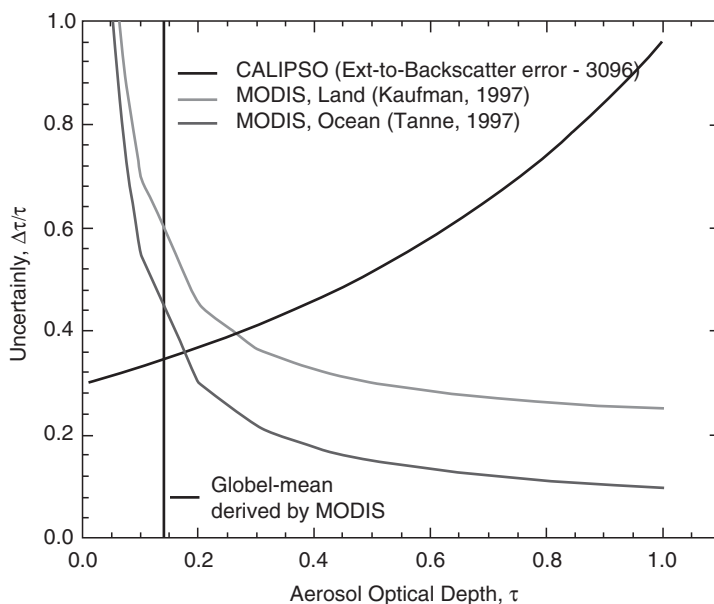


FIGURE 2. Uncertainty estimate for retrieved aerosol optical depth. The CALIPSO algorithm assumes an uncertainty of 30% in the extinction-to-backscatter coefficient. The two different error estimates from MODIS reflect the use of different retrieval techniques for either land or oceanic surfaces.

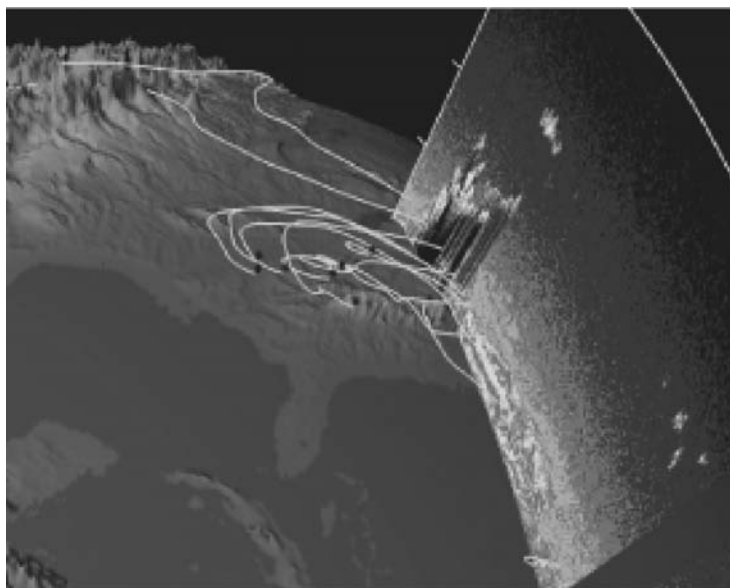


FIGURE 3. Example cross-section of lidar backscatter observations obtained from the LITE experiment over North America. Aerosol layers are denoted by warm colors. Clouds are indicated by white features. The yellow lines are backtrajectories.

theory, ratios approaching unity suggest the presence of larger particles, while those at lower values suggest the presence of smaller particles. This information coupled with absolute backscatter or extinction values can point to the likelihood of cloud, coarse, or fine mode particles. From this data, clouds and aerosols can be separated with confidence as a function of altitude. This capability may prove valuable in tuning of cloud mask algorithms needed for aerosol and cloud retrievals from MODIS and POLDER.

For understanding interactions between aerosols and clouds, CloudSat will provide key information on the properties of optically thick clouds, their ice and liquid water content, and associated rates of precipitation with its 94-GHz radar [Stephens et al., 2002]. Reflectivity measurements will be obtained from the surface to 30 km with 500-m vertical resolution. Because cloud properties can change rapidly, the CloudSat platform will be placed in orbit ~2 minutes behind Aqua, with CALIPSO trailing CloudSat by ~15 sec. In addition, control of CloudSat's cross-track motion will be within ± 1 km of the CALIPSO ground track to ensure the most lidar/radar observations are co-aligned.

Concurrent observations of thermodynamic state parameters (e.g., temperature, relative humidity) from instruments on Aqua will provide the ability to examine interrelationships between aerosol optical depth, single scattering albedo, and relative humidity. Importantly, concurrent A-train aerosol observations with radiative flux measurements from CERES will enable more accurate

TABLE 1. A-Train Instrument Characteristics and Related Products

Spacecraft	Instruments	Characteristics	Aerosol/Cloud Products
Aqua	MODIS	36-channel visible radiometer 2300-km swath Variable pixel resolution .25 to 1 km	Land, ocean, and atmospheric products; include cloud and aerosol optical depths and particle size information
	AIRS/AMSU-A	IR and microwave sounders, 1650-km swath IR pixel resolution ~10 km	Temperature and moisture profiles in clear atmosphere
	AMSR-E	6-channel microwave radiometer 1445-km swath	Liquid water path, column water vapor, liquid precipitation
	CERES	Broadband and spectral radiances converted to fluxes Pixel resolution ~20 km	Top of atmosphere radiation budget Time mean and instantaneous fluxes
	CloudSat	94-GHz radar 500-m vertical range gates from surface to 30 km Pixel resolution ~1.4 km	Cloud profile information, liquid and ice water content, precipitation
CALIPSO	Lidar	532- and 1064-nm channels with depolarization Field of view 70 m at surface with 333-m separation between samples	Aerosol and cloud profile for optically thin clouds Aerosol extinction, optical depth, and typing
	IIR/WFC	3-channel IR radiometer Visible wide field of view camera 64-km swath IR pixel resolution 1 km WFC pixel resolution 125 m within 2.5 km of nadir and 1 km beyond	Cirrus cloud properties
PARASOL	POLDER	9-channel polarimeter with channels in visible and near IR. 400-km swath Pixel resolution 5 km	Cloud and fine mode aerosol optical depth and particle sizes
Aura	HIRDLS	IR limb sounder	Trace gases and stratospheric aerosol
	MLS	Microwave limb sounder	Trace gases, ice content of upper tropospheric cloud
	TES	IR imaging spectrometer Pixel resolution .5 × 5 km	Trace gases
	OMI	UV grating spectrometer Pixel resolution 13 × 24 km	Ozone, aerosol optical depth and single scattering albedo

observationally based estimates of aerosol forcing over the globe. This method has already been demonstrated by Haywood et al. [1999] and Christopher and Zhang [2002] using MODIS/CERES data. The added information from CALIPSO and CloudSat should improve estimates near and in cloudy regions and regions with bright surfaces.

Acknowledgements Some of the data used in this lecture were acquired as part of the NASA's Earth Science Enterprise. The MODIS aerosol retrievals were provided by MODIS Science Teams and data processed by the MODIS Adaptive Processing System (MODAPS). These are archived and distributed by and Goddard Distributed Active Archive Center (DAAC).

References

- Bellouin, N., O. Boucer, D. Tanre and O. Dubovik, Aerosol absorption over the clear-sky oceans deduced from POLDER-1 and AERONET observations, *Geophys. Res. Lett.*, **30**(14), 1748, doi:10.1029/2003GL017121, 2003.
- Charlson, R.J., S.E. Schwartz, J.M. Hales, R.D. Cess, J.A. Coakley, J.E. Hansen, and D.F. Hofmann, Climate forcing by anthropogenic aerosols, *Science*, **255**, 423–430, 1992.
- Coakley, J.A., R.L. Bernstein, and P.A. Durkee, Effect of shipstack effluents on cloud reflectivity, *Science*, **237**, 1020–1022, 1987.
- Husar, R., J.M. Prospero, and L.L. Stowe, Characterization of tropospheric aerosols over the oceans with the NOAA advanced very high resolution radiometer optical thickness operational product, *J. Geophys. Res.*, **102**, 16889–16909, 1997.
- Intergovernmental Panel on Climate Change, Aerosols, their direct and indirect effects, ed., J. Penner et al., *Climate Change 2001, The Scientific Basis. Working Group I to the Third Assessment Report of the IPCC*, Cambridge University Press, 2001.
- Kaufman, Y.J., and T. Nakajima, Effect of Amazon smoke on cloud microphysics and albedo – Analysis from satellite imagery, *J. Appl. Meteor.*, **32**, 729–744, 1993.
- Nakajima, T., A. Kawamoto, and J.E. Penner, A possible correlation between satellite-derived cloud and aerosol microphysical parameters, *Geophys. Res. Lett.*, 2001.
- Remer, L.A., D. Tanre, Y.J. Kaufman, C. Ichoku, S. Mattoo, R. Levy, D.A. Chu, B. Holben, O. Dubovik, A Smirnov, J. Martins, R. Li, and Z. Ahman, Validation of MODIS aerosol retrieval over ocean, *Geophys. Res. Lett.*, **29**, 10.1029/2001GL013204, 2002.
- Stephens, G.L., D.G., Vane, R.J. Boain, G.G. Mace, K. Sassen, Z. Wang, A. Illingworth, E O'Conner, W. Rossow, S. Durden, S. Miller, R. Austin, A. Benedetti, C. Mitrescu, The CloudSat mission and the a-train; a new dimension of space-based observations of clouds and precipitation, *Bull. Amer. Meteor.*, **83**, 12, 1771–1762, 2002.
- Torres, O., R. Decae, and P. Veefkind, OMI Aerosol Retrieval Algorithm. In *OMI Algorithms Theoretical Basis Document, Volume III, Clouds, Aersols, and Surface UV Irradiance*, P. Stammes (ed.), NASA-KNMI, 2002.
- Twomey, S.A., The influence of pollution on the shortware albedo of clouds, *J. Atmos. Sci.*, **34**, 1114–1152, 1977.
- Winker, D.M., J. Pelon, and M.P. McCormick, The CALIPSO mission: Spaceborne lidar for observation of aerosols and clouds, *Proc. SPIE*, **4893**, 1–11, 2003.

Observing Systems for Atmospheric Composition
Satellite, Aircraft, Sensor Web and Ground-Based
Observational Methods and Strategies

Visconti, G.; Di Carlo, P.; Brune, W.; Schoeberl, M.;
Wahner, A. (Eds.)

2007, XII, 244 p. 60 illus., 10 illus. in color., Hardcover
ISBN: 978-0-387-30719-0